Proceedings Paper:

Joyce, R and Zhang, L (2014) The effectiveness of low power co-channel lamppost mounted 3G/WCDMA microcells. In: European Wireless 2014; 20th European Wireless Conference; Proceedings of. 20th European Wireless Conference, 2014, 14-16 May 2014, Barcelona, Spain. VDE , 1 - 6. ISBN 978-3-8007-3621-8

The Effectiveness of Low Power Co-channel Lamppost Mounted 3G/WCDMA Microcells

Robert Joyce
University of Leeds
Leeds, UK
eenrmj@leeds.ac.uk

Li Zhang
University of Leeds
Leeds, UK
l.x.zhang@leeds.ac.uk

Abstract—**This paper considers the effectiveness of low power lamppost mounted 3G/WCDMA microcells to capture traffic when deployed on a common carrier frequency with an overlaying 3G/WCDMA macrocell layer. The paper assesses the potential offload achieved through the deployment of thirteen low power (+24dBm maximum output power) lamppost mounted 3G/WCDMA microcells along a busy street in central London through both simulation and field trials. The paper concludes that low power +24dBm 3G/WCDMA microcells have the potential to significantly offload a co-channel macrocell layer, provided that the microcells are placed in areas of high traffic and are spaced close enough together (<100m) to provide contiguous microcell dominance.**

I. INTRODUCTION

Mobile broadband data traffic is rapidly expanding across the globe as more and more users adopt feature phones, smart phones, connected laptops and tablets [1]. To cope with this so called "data tsunami" Mobile Network Operators (MNOs) are having to rapidly increase the capacity of their cellular networks through the acquisition of more radio spectrum, through the use of more spectrally efficient radio access technologies such as fourth generation networks based on Long Term Evolution (4G/LTE) radio technology and through the deployment of more, and increasingly smaller, radio cell sites within their networks. Given that small cell Base Transceiver Stations (BTSs) will typically have a much lower transmit power than their macrocell equivalents, the cell range of a small cell will be much smaller than that of a macrocell, especially when deployed on a common carrier with the macrocell layer because of the dominant interference from the co-channel macrocell layer.

This paper considers just how effective low power lamppost mounted 3rd Generation Wideband Code Division Multiple Access (3G/WCDMA) microcells will be at capturing traffic from the co-channel macrocell layer. The paper begins with a review of earlier work on macrocell offloading using outdoor microcells and the challenges identified within these references. The paper then models the potential offload achieved by the deployment of thirteen low power (+24dBm maximum output power) lamppost mounted 3G/WCDMA microcells along a busy street in central London through network simulation. The simulation results obtained are then compared to field measurements taken before and after the deployment of four lamppost mounted Alcatel Lucent 3G/WCDMA microcells along Kensington High Street in central London and finally conclusions are drawn as to the effectiveness of low power lamppost microcells at capturing traffic from a co-channel macrocell layer.

II. REVIEW OF PREVIOUS LOW POWER CO-CHANNEL 3G/WCDMA MICROCELL OFFLOAD STUDIES & FIELD TRIALS

There appears to be very little earlier work considering macrocell offload using lamppost mounted low power 3G/WCDMA cells. Some reference regarding offload to higher power street level microcells or indoor femtocells were found and are worthy of consideration since they also address macrocell offloading onto a shared carrier small cell network.

Jami & Tao [2] study co-channel microcell offload in a Release 99 (Rel. 99) 3G/WCDMA network, using high power microcells with an output power of 10W (+40dBm). A modified Walfisch-Ikegami model [3] is proposed based on field measurements made around a single microcell and it is proposed that given these findings a separate model per microcell would be required for accurate microcell coverage prediction. The paper then considers analytically the radius and capacity of a single microcell located at varying distances from a nearby single co-channel macrocell using a Hata based channel model for the macrocell path loss prediction [3]. The paper concludes that for a microcell output power of 10W, the cell radius of the co-channel microcell will be 100m, 150m and 200m at distances of 1km, 1.5km and 2km from the macrocell respectively. While the approach appears sound, there is no mention of the effect of shadowing or penetration loss on the macrocell signal's path loss and therefore it is expected that the cell radii presented will be somewhat smaller than those actually seen from a deployed 10W co-channel microcell.

In a later reference Kim [4] also considers the effect of microcell powers of 1W, 5W, 10W, 15W and 20W on Rel-5 3G/WCDMA microcell radii when the microcell is deployed on a shared carrier with the macrocell layer. Unfortunately it appears that the paper does not model the High Speed Downlink Packet Access (HSDPA) downlink SINR correctly since values as high as 70dB are presented and since 3G/WCDMA uses co-channel common channels, then even with good orthogonality between the downlink channels an HSDPA SINR much above 25dB is unlikely to be seen in a deployed network. Even so the paper shows that the further from the co-channel macrocell the microcell is placed the better the microcell throughput, with HSDPA microcells at 900m from the macrocell achieving over twice (2.1Mbps) the capacity of microcells located at 300m from the macrocell (1.0Mbps).

Erceg & Whitehead [5] estimate, purely from field measurements, the cell size that can be achieved from lamppost mounted small cells operating in the 900MHz, 2GHz and 6GHz frequency bands for US 1G Advanced Mobile Phone Service [6], 2G/IS-54 [7] and 2G/IS-95[8] cellular systems. The reference also considered capacity limited ranges for a given user distribution and suggests that powers as low as +5dBm power may be suitable for street level coverage at 2GHz for an interference limited microcell only network.

References [9,10] look at the offloading of the macrocell network through indoor femtocell rather outdoor microcell deployment using a simulation approach with a Shannon based throughput C/I mapping very similar to that used in the simulations presented in this paper. It is shown that femtocells can operate on a shared carrier with very little uplink interference into the macrocell network. The work concludes that offloading a single deep indoor user from the macrocell provides up to 2.5 times its capacity for outdoor users and that for the scenarios studied the co-channel deployment of femtocells not only offloaded the macros but also provided what was termed in the paper an "offloading capacity gain" on the macrocells of between 30-100%.

Finally reference [11] evaluates through field measurement the effectiveness of low power (+13dBm) co-channel indoor 3G/WCDMA femtocells to provide coverage to a dense urban environment. Simultaneous field measurements of both 3G/WCDMA (2100MHz) and IEEE 802.11 Wi-Fi (2.4GHz) networks are taken throughout central Vienna and the signal levels seen at 540 distinct locations throughout the city are analysed. It is shown that given the proliferation of Wi-Fi access points, for central Vienna at around 55% of sample location the Wi-Fi signal is stronger than the 3G/WCDMA signal. At these locations it is proposed that the deployment of a femtocell alongside the associated Wi-Fi access point would provide better coverage for the 3G/WCDMA users than that currently provided by the macrocell layer. The paper provides both a method for the placement of indoor small cells and also suggests that low power +13dBm outdoor small cells may also be effective in offloading traffic from the macrocell layer.

In summary many papers were found regarding offload from the 3G/WCDMA macrocell layer to co-channel indoor femtocells, a number of papers were found that considered the cell size of outdoor lamppost mounted microcells but did not consider explicitly the actual traffic offloaded onto these microcells.

III. Output Power Considerations For Lamppost Mounted Small Cell Deployments

Using the Urban Micro Outdoor to Indoor propagation model proposed in 3GPP 25.814 [12] to predict the coverage from the low powered small cells and assuming dominance occurs when the Received Signal Code Power (RSCP) of the microcell is greater than the average RSCP of the dominant overlaying macrocell, results in the following cell sizes shown in Fig. 1 for microcells with output powers ranging from +10 (10mW) to +37dBm (5W) for the co-channel deployment case. From the figure it is seen that the small cell's size is not only a function of output power of the small cell but also the level of interference seen from the surrounding co-channel macrocell layer. For example, for a +24dBm output power small cell its effective cell size (with indoor penetration loss - since this was included in the 3GPP 25.814 model used) will range from 20m to 60m when deployed in an environment with a macrocell RSCP power range of -60dBm to -90dBm. While these sizes initially appear very limited it should also be remembered that the spacing between lampposts can be as low as 10m in an urban environment and outdoor coverage ranges will be significantly larger than the indoor ranges given above and therefore it would appear from the graph below that co-channel small cell dominance should still be possible using output powers as low as +10dBm providing that the lamppost spacing chosen between the small cells is adequate for the level of macrocell interference experienced in the area of small cell deployment.

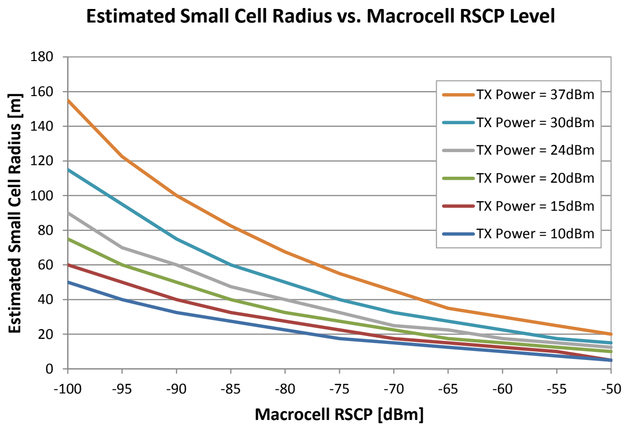

Fig. 1. Estimated co-channel small cell size vs. macrocell RSCP level using the 3GPP 25.814 urban micro outdoor to indoor propagation model for different small cell transmitter powers.

IV. Telefonica UK Kensington High Street Microcell Network

Telefonica UK deployed over 100 outdoor 3G/Wi-Fi small cell access points into central London throughout 2012 [13] in readiness for the anticipated mobile data traffic increase during the London 2012 Olympics games. Deployment was focused on areas with high 3G traffic levels as reported from network statistics. The remainder of this paper focuses only on the small cell network deployed along Kensington High Street (KHS) since this has been used by Telefonica UK as its small cell testbed and far more measurements and observations have been made of this area than any of the other small cell deployment areas.

The KHS small cell network consists of thirteen 3G/Wi-Fi microcells deployed upon existing lampposts along a 1.4km stretch of KHS, with the inter-site distances between the chosen lampposts ranging from 60 to 100m. The layout of the KHS microcell network is shown in Fig. 2 which also shows the position of the surrounding macrocell sites in relation to the KHS small cell network. Each KHS small cell consists of a hybrid 3G/Wi-Fi microcell located at a height of 8m on an existing KHS lamppost. The Wi-Fi Access Point was a Ruckus Wireless 8800 and the 3G microcell unit was an Alcatel Lucent Metro V2 outdoor microcell BTS with an output power of +24dBm. Based on a design proposed by the Telefonica both units were mounted back to back using a special mounting bracket developed by Ruckus Wireless (Fig. 3) and when mounted together appeared as an integral single unit.

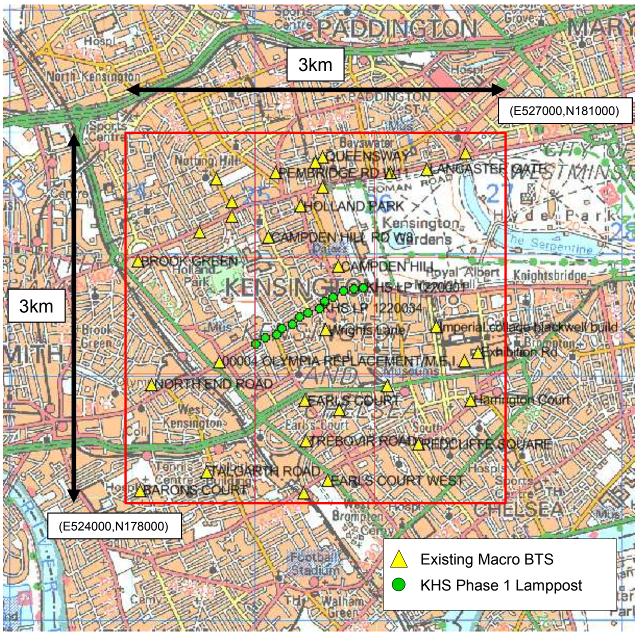

Fig. 2. Map showing KHS microcell network in relation to existing macrocells and the 3x3km Kensignton simulation area.

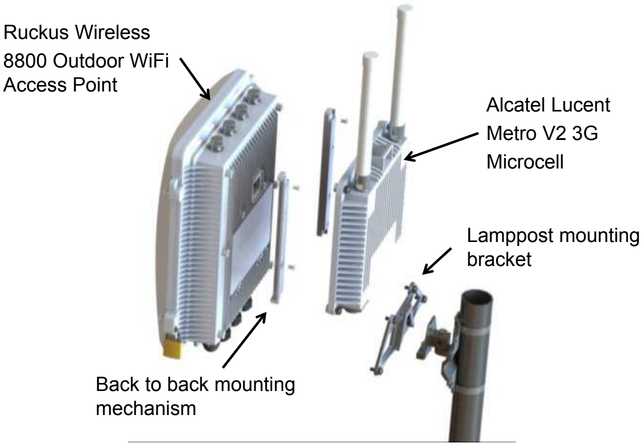

Fig. 3. Exploded schematic of the Telefonica 3G/Wi-Fi microcell.

V. Microcell Network Simulation & Predicted Traffic Offload

This section considers through simulation the expected coverage and traffic offload that the KHS microcells would provide. Simulations were performed for the KHS small cell network using a bespoke 3G/4G Network Simulator developed at the University of Leeds. Building penetration loss was derived from London land use clutter data made available by Telefonica UK (Fig. 4) and a special clutter category (category 17) was used to define the KHS high traffic areas within the simulation area (KHS clutter area = 0.1225km^2). The users/km^2 applied for each clutter category, normalised to equal the total number of users distributed for each simulation, is given in Table I. The penetration loss for the KHS clutter category was set to 16dB, the same as for the Dense Suburban clutter surrounding the KHS area. The penetration losses assumed within the Network Simulator for the other clutter categories are also shown in Table I.

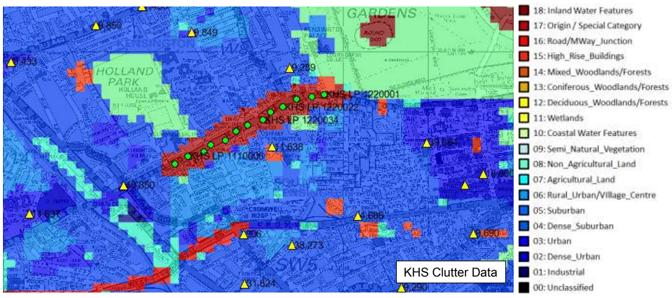

Fig. 4. Clutter Categories for Kensington small cell simulation area — showing the use of clutter category 17 to define the KHS high traffic area surrounding the thirteen lamppost microcells.

TABLE I. Assumed Penetration Loss & Nominal Traffic Density For Each Clutter Category Within Simulation Area.

Clutter Category	Description	Penetration Loss [dB]	Users/km^2
0	Unclassified	0	0
1	Industrial	14	100
2	Dense Urban	24	300
3	Urban	20	200
4	Dense Suburban	16	100
5	Suburban	14	50
6	Rural Urban/Village Centre	8	10
7	Agricultural Land	0	10
8	Non Agricultural Land	0	10
9	Semi Natural Vegetation	2	10
10	Coastal Water Features	0	10
11	Wetlands	0	10
12	Deciduous Woodlands/Forests	4	10
13	Coniferous Woodlands/Forests	4	10
14	Mixed Woodlands/Forests	4	10
15	High Rise Buildings	16	400
16	Road/Motorway Junction	6	200
17	Origin/Special Category	0/16(KHS)	1500
18	Inland Water Features	0	50

A. KHS Macro and Microcell Coverage Predictions

The Network Simulator was used to predict the coverage of both the macrocells and the lamppost microcells along and around KHS for the co-channel case. The propagation model used for the macrocells was the 3GPP 25.814 “Macrocell distance-dependent path loss model” [12] and the microcells’ coverage was predicted using the 3GPP 36.814 “Urban Micro Line of Sight (LoS) propagation model” [14]. A clutter based penetration loss was applied in both cases. Shown in Figs. 5

and 6 are the best server RSCP coverage plots for the case with and without the KHS microcells deployed. In Fig. 5 the cell identities, sector numbers and the scrambling codes for the nearby surrounding sectors area also given.

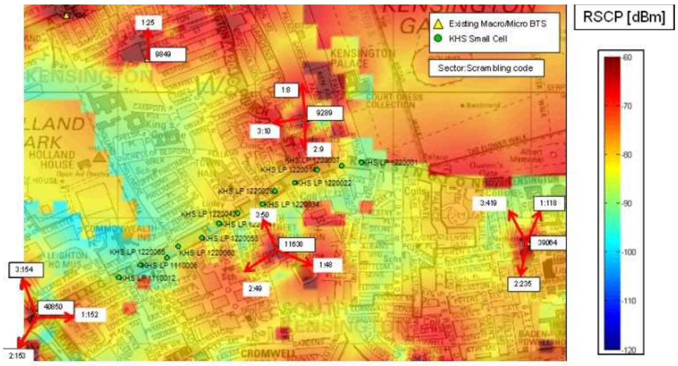

Fig. 5. Simulated macrocell best server RSCP coverage along KHS prior to activation of KHS microcells. Also shown are the cell identities, sector identities and scrambling codes for the macrocell sectors closest to KHS.

Fig. 6. Simulated macrocell & microcell best server RSCP coverage along KHS following activation of the thirteen +24dBm KHS microcells.

B. *KHS Microcell Traffic Offload Predictions*

The results of the coverage predictions were then used to perform simulations to estimate the amount of traffic offloaded from the surrounding macrocells onto the KHS microcells. Monte Carlo simulation runs were performed with and without the KHS microcells active for 1,000 Monte Carlo snap shots each with an arbitrary 500 users distributed according to clutter category across the entire 3x3km simulation area. Of the 500 users distributed, normalised clutter spreading led to 92 out of the 500 users being distributed within the 0.1225km^2 KHS high traffic area leading to an average user density of 751 users/km^2 within the KHS high traffic area and 105 users/km^2 on average in the surrounding macrocell served area. Cell and user statistics were gathered from the simulations for both the central 2x2km area and the KHS high traffic area.

Shown in Fig. 7 is a graph showing the predicted change in the coverage areas of the five dominant macrocell sectors covering the KHS high traffic area, before and after the deployment of the thirteen KHS microcells. Also shown in the graph is the total combined coverage area of all the microcells when deployed. It can be seen from the graph that the combined coverage footprint of the microcells (0.3768 km^2) is significantly bigger than KHS high traffic area (0.1225km^2).

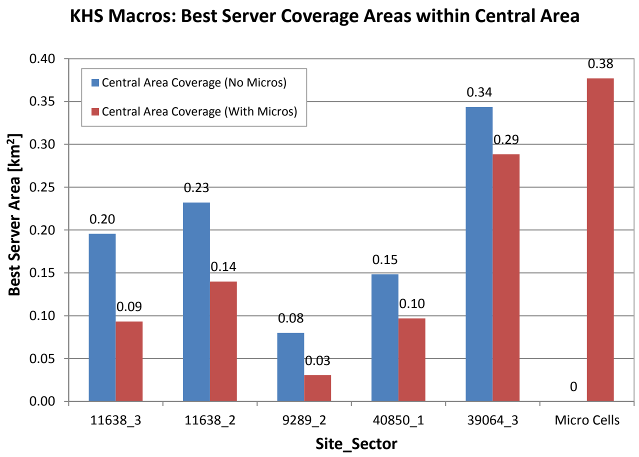

Fig. 7. Predicted best server areas of the five dominant macrocells before and after the deployment of the thirteen KHS microcells. Also shown is the predicted combined coverage area of the KHS microcells.

While the reduction in the best server area for most of the KHS serving macrocell sectors is around 50%, since the users within the simulation are not evenly distributed but skewed towards the KHS high traffic area, the introduction of the microcells has a much more dramatic effect on the number of users served by each of the five dominant macrocell sectors (Fig. 8). Here it can be seen that all of the dominant five serving macrocell sectors experience a significant reduction in the number of served users with the introduction of the KHS microcells.

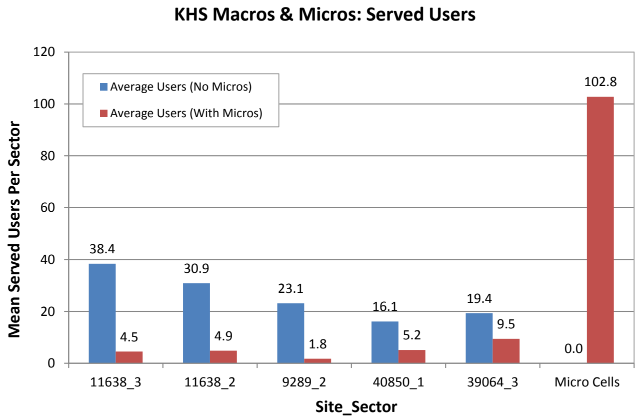

Fig. 8. Predicted users served for the five dominant macrocell sectors before and after the deployment of the thirteen KHS microcells. Also shown is the predicted users served across all thirteen of the KHS microcells following their deployment.

While from the above results it appeared that the Monte Carlo simulations predict that the +24dBm microcells would have dominant coverage on KHS and that they will also capture a significant number of users from the macrocell layer, the key question still to be answered was how would the microcell deployment enhance the user experience in KHS and across the wider network? An overall summary of the gains and losses predicted by the simulation of the KHS microcell deployment is given in Table II.

From a radio coverage perspective the microcells have little change on the average RSCP and Ec/Io across the central 2x2km area of the simulation area. The reduction in Ec/Io is due to the increased number of pilots seen around KHS, and while this does have a slight negative effect on the average throughput per sector of the surrounding macrocells, because there are now fewer users on these surrounding macrocells, the average user throughput seen on these surrounding macrocells actually increases from 0.27Mbps to 0.36Mbps following microcell deployment. Overall the KHS microcells offload on average 102.8 users from the macrocell layer and this leads to a 22.49Mbps increase in total network throughput, representing a 22% increase in the capacity of the network. The most significant impact of the microcells however is the effect they have on the user experience for the users located in the KHS high traffic area. Prior to the deployment of the microcells, these users experienced an average throughput of just 0.08Mbps, whereas after deployment their average throughput of 0.26Mbps is more in line with the average throughput seen by the surrounding macrocell users.

Simulation result therefore suggest that +24dBm microcells will provide contiguous coverage dominance along KHS and if there is significant traffic within this area they will also provide significant traffic offload from the surrounding macrocell sectors.

TABLE II. SUMMARY OF KHS MICROCELL SIMULATION RESULTS.

Central 2x2km Area			
Key Performance Indicator	Macros Only	Macros & Micros	Gain/Loss
Mean RSCP [dBm]	-78.90	-78.06	0.85
Mean Ec/Io [dB]	-11.21	-11.49	-0.28
Macro Network Throughput [Mbps]	101.99	99.30	-2.69
Network Throughput (Macro & Micro) [Mbps]	101.99	124.48	22.49
Mean Macro Sector Throughput [Mbps]	2.32	2.26	-0.06
Mean Macro Users Per Sector [Users]	8.63	6.30	-2.33
Mean Macro User Throughput [Mbps]	0.27	0.36	0.09
Mean Users In Central Area on Macros [Users]	379.84	277.10	-102.74
Mean Macro & Micro User Throughput [Mbps]	0.27	0.34	27%

KHS High Traffic Area			
Key Performance Indicator	Macros Only	Macros & Micros	Gain/Loss
Micro Network Throughput [Mbps]	-	25.18	25.18
Mean Micro Sector Throughput [Mbps]	-	1.87	1.87
Mean Micro Users Per Sector [Users]	-	7.68	7.68
Mean Users Microcell Layer [Users]	-	102.80	102.80
KHS Area Mean User Throughput [Mbps]	0.08	0.26	218%

VI. KENSINGTON HIGH STREET MICROCELL MEASUREMENTS

In order to validate the actual effectiveness of the KHS microcells a number of field measurements were performed by Telefonica UK before and after the activation of the initial 3G/WCDMA KHS microcells. At the time of writing while all thirteen KHs microcells have been enabled for Wi-Fi service, only four have been enabled for 3G/WCDMA service due to backhaul transmission issues. However, RF measurements have been performed on the initial four 3G/WCDMA microcells deployed and this section outlines the measurements performed and analysis undertaken on these measurements.

Drive surveys were performed using a PCTEL Seagull EX radio scanner following the activation of the initial four 3G/WCDMA microcells (LP1220001, LP1220007, LP1220022 and LP1220029). Shown in Fig. 9 is a plot showing the best server areas for the section of KHS over which active 3G microcells were dominant together with the length of KHS over which each of the microcells was the dominant server. The maximum length of KHS over which a microcell was dominant was 250m (L1220001) and the minimum length was 115m (L1220022). From the figure it can also be seen that continuous dominance along KHS is not actually fully achieved by the four microcells deployed, with sector 9289_2 achieving dominance for a short distance (25m) between lampposts LP1220014 and LP1220022. This was due to the lack of coverage from the missing microcell on lamppost LP1220014 and as was shown earlier in the macrocell coverage plot (Fig. 5), it is this precise area where the most interference from the macrocell network was expected to occur and in particular interference from sector 9289_2. However, it is also worth mentioning that given significant traffic may be offloaded from the macrocell layer, then in some cases for example in the case of sector 9289_2, where significant traffic is expected to be offloaded from the sector, yet the sector still causes unwanted interference, it may be possible to alleviate this interference by reducing the power or changing the antenna tilt or both for the co-channel carrier of sector 9289_2.

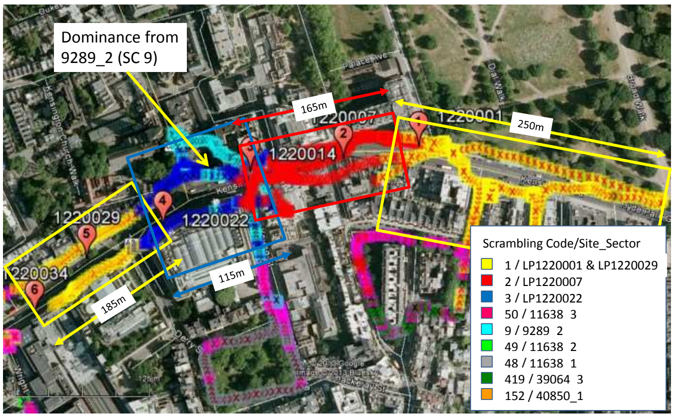

Fig. 9. Best server scrambling code plot for the F2 carrier for the section of KHS over which 3G/WCDMA microcells were the dominant servers.

The graph presented in Fig. 10 shows the measured best server RSCP before and after the activation of the initial four microcells and the predicted coverage from the five lampposts microcells LP1220001, LP1220007, LP1220014, LP1220022 and LP1220029 using the "Urban Micro LoS propagation model" given in [14]. Here it can be seen the four active microcells provide significant dominance over the macrocell coverage as predicted by the earlier simulations. The predicted coverage from the microcell LP1220014, also shows that complete coverage dominance is expected to be achieved between microcells LP1220007 and LP1220022 once LP1220014 is activated for 3G/WCDMA service. Although predicted signal levels of -40dBm were not measured from the microcells during the surveys, this was not a surprise since the 3GPP model does not take into account any shadowing or reduction in the antenna gain of the microcell seen when directly underneath the microcell. Further out the line of sight microcell measurements appear to match well with the 3GPP microcell LoS model used. As predicted by this model and also measured in the field, +24dBm low power lamppost mounted microcells do provide dominance and have the potential for significant traffic capacity offload when deployed on a shared carrier with the macrocell layer providing that they are spaced close enough together to overcome the co-channel interference from the macrocell layer.

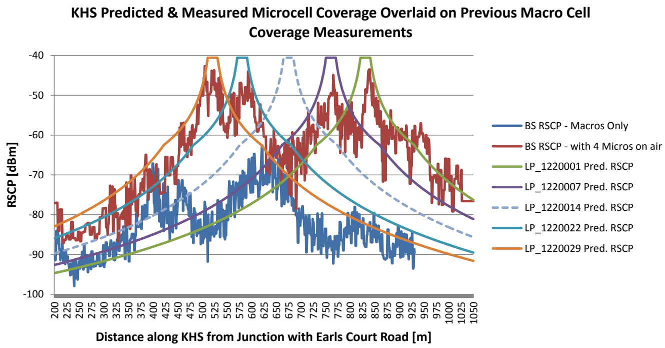

Fig. 10. Best server scrambling code plot for the F2 carrier for the section of KHS over which 3G/WCDMA microcells were the dominant servers.

VII. CONCLUSIONS

This paper has presented work undertaken to understand the effectiveness of low power lamppost mounted 3G/WCDMA microcells to capture traffic from a co-channel macrocell layer. Simulations and measurements have been undertaken for a 3G/Wi-Fi small cell network deployment on thirteen lampposts along Kensington High Street, London. Both modelling and simulations have suggested that dominance can be achieved by +24dBm 3G/WCDMA microcells when deployed under a co-channel macrocell layer and it has been shown that the microcell range obtained depends primarily on the level of interference from the macrocell layer. Typical outdoor to indoor microcell radii predicted from modelling and simulation assuming a 20dB building penetration loss range from 30 to 90m, however it is also expected that the outdoor microcell range would be much greater than this. Simulations were also performed to study the potential of the 3G/WCDMA microcells to offload traffic from the macrocell sectors surrounding the area of KHS. These simulations suggested that a proposed network of thirteen low power 3G/WCDMA microcells would indeed capture significant traffic from the surrounding macrocells providing that traffic was located on or close to KHS.

Finally a series of RF measurement drive surveys were conducted before and after the activation of the initial four 3G/WCDMA microcells in order to validate the macro and microcell coverage simulations and to measure the effective dominance area of the microcells once they had been activated. Analysis of the drive survey measurements showed that the active 3G microcells clearly provided dominance along KHS and that when all thirteen microcells are enabled for 3G service then contiguous 3G microcell dominance along KHS is expected.

It is therefore concluded that from modelling, simulation and measurements that low power +24dBm 3G/WCDMA microcells do have the potential to significantly offload a co-channel macrocell layer, provided that the microcells are placed in areas of high traffic and are spaced close enough together (<100m) to provide contiguous microcell dominance.

REFERENCES

[1] GSMA, "The Mobile Economy 2013," GSMA, London, 2013.

[2] I. Jami and H. Tao, "Micro-cell planning within macro-cells in UMTS: Downlink analysis," *Proc. Third International Conference on 3G Mobile Communication Technologies,* London, 2002, pp. 211-215.

[3] European Union, "COST 231 final report: digital mobile radio towards future generation systems", chapter 4 propagation prediction models, 1996.

[4] C. Y. Kim, "The evaluation of HCS scenarios included in HSDPA," *Proc. IEEE Vehicular Technology Conference-Fall*, Los Angeles 2004, pp. 4772-4776.

[5] V. Erceg and J. F. Whitehead, "Microcell Size and Architecture Analysis from the Propagation and Capacity Points-of-View," *Proc. IEEE Vehicular Technology Conference*, Stockholm, 1994, pp. 215-219.

[6] W. R. Young, "Advanced Mobile Phone Service - Introduction, Background, and Objectives," *Bell System Technical Journal,* vol. 58, pp. 1-14, 1979.

[7] M. Bezler *et. al.*, "Comparison of Spectrum Efficiency in Digital Cellular-Systems - GSM and Amps-D," *Proc. IEEE Vehicular Technology Conference*, Denver, 1992, pp. 1008-1011.

[8] K. S. Gilhousen *et. al.*, "On the Capacity of a Cellular CDMA System," *IEEE Trans.Vehicual Technology,* vol. 40, pp. 303-312, May 1991.

[9] H. Claussen and D. Calin, "Macrocell Offloading Benefits in Joint Macro- and Femtocell Deployments," *Proc. IEEE 20th International Symposium on Personal, Indoor and Mobile Radio Communications*, Tokyo, 2009, pp. 350-354.

[10] D. Calin *et. al.*, "On Femto Deployment Architectures and Macrocell Offloading Benefits in Joint Macro-Femto Deployments," *IEEE Communications Magazine,* vol. 48, pp. 26-32, Jan 2010.

[11] P. Fuxjager *et. al.*, "Measurement-Based Small-Cell Coverage Analysis for Urban Macro-Offload Scenarios," *Proc. IEEE Vehicular Technology Conference-Spring*, Budapest, 2011, pp. 1-5.

[12] *3GPP Physical layer aspects for evolved Universal Terrestrial Radio Access (UTRA) (Release 7)*, 3GPP 25.814, v7.1.0, 2006.

[13] R. M. Joyce and S. Brown, "Delivering Small Cells into the Heart of London," presented at the Small Cells World Summit 2012, London, 2012.

[14] *3GPP Evolved Universal Terrestrial Radio Access (E-UTRA); Further advancements for E-UTRA physical layer aspects (Release 9)*, 3GPP 36.814, v9.0.0, 2010.